



ISSN 0975-413X  
CODEN (USA): PCHHAX

Der Pharma Chemica, 2017, 9(9):64-75  
(<http://www.derpharmachemica.com/archive.html>)

## An Overview of Picric Acid

Srivastava KK<sup>1</sup>, Shubha Srivastava<sup>1</sup>, Md Tanweer Alam<sup>2</sup>, Rituraj<sup>1</sup>

<sup>1</sup>Department of Chemistry, Vinoba Bhave University, Hazaribagh, India

<sup>2</sup>Department of Chemistry, KBW College, Hazaribagh, India

### ABSTRACT

This paper presents an overview of picric acid. In this review, we summarize the methods of preparation, spectral data, uses, identifiers, chemical properties, hazards and explosive data of picric acid. The interpretation of FTIR data, biological degradation and analytical importance have reviewed and discussed. The experimental and optimized geometrical parameters of picric acid reported have been reviewed. The various aspects of charge transfer complexes of Picric acid as an acceptor reported earlier on the experimental and computational methods have also been reviewed.

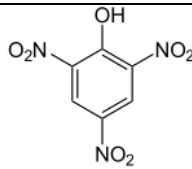
**Keywords:** Picric acid, Picrates, Druggability, Toxicity, Hazards, Computational

Picric acid (*pik' ros* meaning "bitter", reflecting its bitter taste), also known as carbazotic acid, phenol trinitrate, picronitric acid, trinitrophenol, 2,4,6-trinitro-1-phenol, 2-hydroxy-1,3,5-trinitrobenzene, 2,4,6-Trinitrophenol (TNP), Melinite, Pikrinsäure, acide picrique was probably first mentioned in the alchemical writings of Johann Rudolf Glauber in 1742. Peter Woulfe in 1771 synthesized it for the first time from indigo in 1771 [1]. Its synthesis from phenol and the correct determination of its formula were successfully accomplished in 1841 [2].

TNP is a yellow crystalline, bitter [3,4], toxic [5-7], explosive solid [8] which is widely used in the identification of activated compounds in the labs [9], picric acid is also used in medicinal formulations in the treatment of malaria, trichinosis, herpes and smallpox and antiseptics [10], preparation of charge transfer complexes [11-15] of various utilities etc. It has been used as an explosive [8], dyes [16] and antiseptic [10]. In analytical chemistry TNP is used as a test reagent, e.g. to identify alkaloids, cardenolids and creatinine. Further, it is used for colorimetric determination of blood sugar and by microanalysis of carbon steel as Igewesky's Reagenz. Fused aromatics are identified with TNP by formation of colored charge-transfer complexes [16].

TNP is industrially produced by treating phenol with concentrated sulfuric acid and subsequently with nitric acid. In the first reaction phenol is sulfonated, in the following step the sulfonic groups are replaced by nitro groups. An alternative way of synthesis is dinitration of chlorobenzene, followed by hydrolysis to 2,4-Dinitrophenol (DNP) and further nitration to TNP by nitric acid [17]. During the production of nitrobenzene from benzene, TNP and DNP are generated as off-stream chemical, which accumulate in industrial waste waters. Its identifiers appear in Table 1.

**Table 1: Identifiers of picric acid**

Structure	
CAS Registry Number	88-89-1
ChEBI	CHEBI:46149
ChEMBL	ChEMBL108541
ChemSpider	6688
DrugBank	DB03651
InChI[show]	
PubChem	6954
RTECS number	TJ7875000
SMILES[show]	
UNII	A49OS0F91S

Its properties appear in Table 2, while the explosive data appear in Table 3. Table 4 incorporates the hazards of TNP.

Table 2: Properties of picric acid

Chemical formula	C <sub>6</sub> H <sub>3</sub> N <sub>3</sub> O <sub>7</sub>
Molar mass	229.10 g·mol <sup>-1</sup>
Appearance	Colorless to yellow solid
Density	1.763 g·cm <sup>-3</sup> , solid
Melting point	122.5°C (252.5 °F; 395.6 K)
Boiling point	>300°C (572 °F; 573 K) Explodes
Solubility in water	12.7 g·L <sup>-1</sup>
Vapor pressure	1 mmHg (195°C) [1]
Acidity (pKa)	0.38

Table 3: Explosive data of picric acid

Energy of formation	-1014.5 kJ/kg		
Enthalpy of formation	-1084.8 kJ/kg		
Oxygen balance	-45.4%		
Nitrogen content	18.34%		
Volume of explosion gases	826 l/kg		
Heat of explosion			
(H <sub>2</sub> O liquid)	3437 kJ/kg		
(H <sub>2</sub> O gas)	3350 kJ/kg		
Specific energy	995 kJ/kg		
Density	1.767 g/cm <sup>3</sup>		
Solidification point	252.5 °F		
Heat of fusion	76.2 kJ/kg		
Specific heat	1.065 kJ/kg		
Vapour pressure			
	Pressure	Temperature	
	Millibar	°C	°F
	0.01	122	252
	2.7	195	383
	67	255	491
Lead block test	315 cm <sup>3</sup> /10 g		
Detonation velocity, confined	7350 m/s at ρ=1.7 g/cm		
Deflagration point	300°C		
Impact sensitivity	7.4 Nm		
Friction sensitivity	Upto 353 N		
Pistil load no reaction			
Critical diameter of steel sleeve test		4 mm	

Table 4: Hazards of picric acid

Main hazards	Explosive
EU classification	T  E  F+ 
R-phrases	E
S-phrases	R1 R4 R11 R23 R24 R25
	S28 S35 S37 S45
NFPA 704	
Flash point	150°C; 302 °F; 423 K [1]
Lethal dose or concentration (LD, LC):	
LDLo (Lowest published)	100 mg/kg (guinea pig, oral)
	250 mg/kg (cat, oral)
	120 mg/kg (rabbit, oral) [2]
US health exposure limits (NIOSH)	
PEL (Permissible)	TWA 0.1 mg/m <sup>3</sup> [skin]
REL (Recommended)	TWA 0.1 mg/m <sup>3</sup> ST 0.3 mg/m <sup>3</sup> [skin] [1]
IDLH (Immediate danger)	75 mg/m <sup>3</sup> [1]

The experimental characteristic infrared frequencies (cm<sup>-1</sup>) and their assignments appear in Table 5.

Kraus and Fassel [18] have studied regularities in the infrared spectra of forty picric acid molecular complexes and concluded that picric acid (Figure 1) contains three nitro groups where stretching frequencies are not expected to be equivalent.

One nitro group ortho to phenolic-OH is involved in the hydrogen bond with that group. As a result of this interaction, the asymmetrical stretching frequency of nitro group is rotated out of the plane of the ring because of steric- effect of -OH group. The para nitro group is coplanar with the ring as is one of the ortho nitro group but it is not involved in the intra-molecular H-Bonding. The three nitro group asymmetrical stretching frequencies are not resolved and appears as one broad band with maximum at 1529 cm<sup>-1</sup>.

Table 5: IR frequencies and assignments of picric acid

Picric acid	Assignment
3108 s, br	vO-H
2875 w	vs(C-H)
1630vs	vasy NO <sub>2</sub>
1606 ms	vC=CAr
1437 ms	
1341 vs	vs(C-N)
1275 vs	vC-O
1154 ms	vC-H in plane bending
1083 ms	
779 sharp	vC-NO <sub>2</sub> -str
vms	NC-C
703 ms	vC-Hout of plane bending
663 w	vNO <sub>2</sub> wagging

s: Strong; w: Weak; m: Medium; sh: Shoulder, v: Very; vs: Very strong; br: Broad n stretching vs symmetrical stretching vasy asymmetry

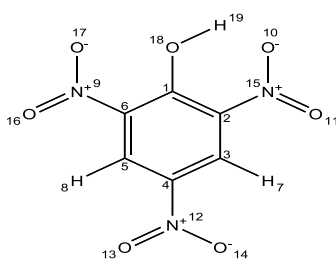


Figure 1: Structure of picric acid

## (a) Assignment of the RR spectra of solid state picric acid

Experimental RR spectra of deep yellow picric acid are compared (Figure 2) with a computed (DFT) spectrum is shown in Figure 3.

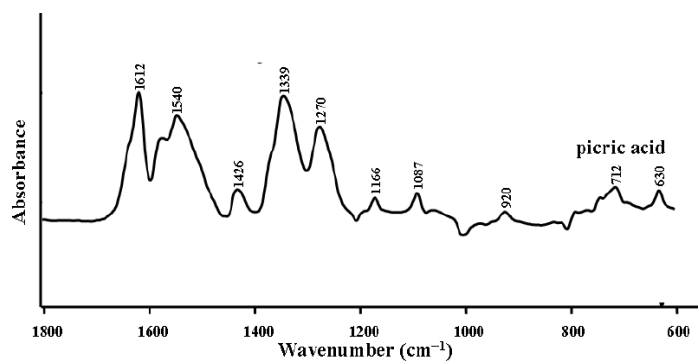


Figure 2: ATR/ FTIR spectra of picric acid

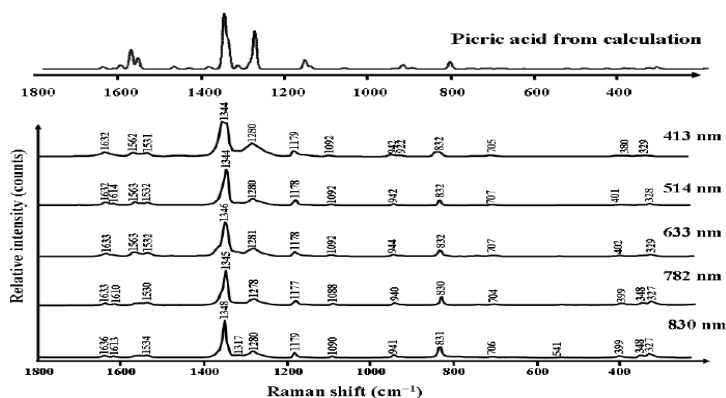


Figure 3: RR spectra of picric acid

Observed and computed wavenumber values are listed in Tables 6 and 7 respectively.

**Table 6: Observed Raman bands ( $\text{cm}^{-1}$ ), assignments, symmetry terms, and local coordinates for picric acid at 413, 514, 633, 782 and 830 nm Excitation**

Picric acid					Local coordinate
413	514	633	782	830	
1632	1632	1633	1633	1636	CC ring str
1614	1610	1613			$\nu(\text{NO}_2)$ asym
1562	1563	1563			
1531	1532	1532	1530	1534	
1344	1344	1346	1345	1348	$\nu(\text{NO}_2)$ sym
1280	1280	1281	1278	1280	$\nu(\text{NO}_2)$ sym
1179	1178	1178	1177	1179	sym CN str
1092	1092	1092	1088	1090	
942	942	944	940	941	
832	832	832	830	831	$\delta(\text{NO}_2)$ in-plane (scissoring)

The bands at 1610, 1345 and  $830\text{ cm}^{-1}$  were assigned to the anti-symmetric stretch, symmetric stretch and in-plane (scissoring) deformation, respectively of the aromatic  $\text{NO}_2$  groups of picric acid. The exact position of the in-plane  $\text{NO}_2$  wagging deformation cannot be verified [19], however in this work, a broad band at  $722\text{ cm}^{-1}$  was expected. Raman wavenumber value of the  $\text{NO}_2$  group of picric acid at 1614 and  $1345\text{ cm}^{-1}$ , respectively.

**Table 7: Calculated Raman Bands ( $\text{cm}^{-1}$ ) for selected vibrational modes of picric acid at 2 Levels: B3LYP/6-311+G\***

Band position/ $\text{cm}^{-1}$ a scale	IR ( $\text{int}/\text{km mol}^{-1}$ )	Raman activity/ $\text{A}^4\text{u}^{-1}$	Band assignment
768.6	43.8	2.1	HO out of plane def
814.6	0.3	22.8	in plane ring def +d (ONO) sym
812.2	2.3	3.8	d (ONO) para (+in plane ring def)
906.2	64.9	5	ortho CN antisym str
927.7	31.9	15.7	para CN str (+other 2)
940.5	17.5	1.1	CH out of plane (sym)
948.8	0.8	2.1	CH out of plane (anti)
1068.5	88	3	CH in plane bend (clap)
1150.5	44.2	9.7	CH & OH in plane bend (clock)
1163.4	16.7	33.3	sym CN str (all 3)
1283.9	157.7	139.9	$\text{NO}_2$ str (H-bonded ortho) + OH & CH bends
1295.7	102.1	22.7	OH & CH bends

Ramalingam et al. [20] have carried out DFT study on picric acid on Gaussian 03 program package and has reported the optimized bond length (in Å) and bond angle of Picric acid using PB3LYP/6311G (d,p) and 6311 GDP level of theory. The observed and calculated values of bond length, bond angle and dihedral angle have been summarized in the Tables 8-10.

**Table 8: Observed and calculated bond length (Å) of picric acid**

Geometrical parameters bond length	Methods					Experimental value
	HF	B3LYP		B3PW91		
	6-311G (d,p)	6-31G (d,p)	6-311G (d,p)	6-31G (d,p)	6-311G (d,p)	
C1-C2	1.408	1.42	1.416	1.418	1.414	1.392
C1-C6	1.41	1.426	1.423	1.424	1.42	1.406
C1-O18	1.299	1.315	1.315	1.31	1.31	1.357
C2-C3	1.371	1.382	1.379	1.38	1.377	1.402
C2-N9	1.458	1.475	1.482	1.47	1.475	1.451
C3-C4	1.385	1.394	1.391	1.392	1.389	1.384
C3-H7	1.071	1.082	1.081	1.083	1.082	1.08
C4-C5	1.371	1.383	1.38	1.381	1.378	1.387
C4-N12	1.451	1.469	1.477	1.464	1.471	1.451
C5-C6	1.384	1.391	1.389	1.389	1.386	1.383
C5-H8	1.07	1.082	1.08	1.083	1.082	1.08
C6-N15	1.449	1.457	1.465	1.451	1.458	1.451

N9-O10	1.194	1.229	1.222	1.224	1.216	1.225
N9-O11	1.186	1.224	1.216	1.218	1.211	1.217
N12-O13	1.192	1.228	1.221	1.223	1.215	1.225
N12-O14	1.191	1.228	1.221	1.222	1.215	1.217
N15-O16	1.183	1.219	1.212	1.214	1.206	1.225
N15-O17	1.206	1.251	1.243	1.245	1.238	1.217
O17-H19	1.782	1.646	1.676	1.625	1.649	-
O18-H19	0.953	0.994	0.987	0.995	0.989	0.82

Table 9: Observed and calculated bond angle of picric acid

Geometrical parameters bond angle (Å)	Methods					Experimental value
	HF	B3LYP		B3PW91		
	6-311G (d,p)	6-31G (d,p)	6-311G (d,p)	6-31G (d,p)	6-311G (d,p)	
C2-C1-C6	115.84	115.83	115.72	115.77	115.64	-
C2-C1-O18	119.31	120.82	120.34	120.97	120.55	-
C6-C1-O18	124.8	123.31	123.91	123.22	123.77	-
C1-C2-C3	122.49	122.08	122.34	122.09	122.35	-
C1-C2-N9	120.81	121.03	120.66	121.01	120.65	-
C3-C2-N9	116.69	116.87	116.99	116.88	116.98	-
C2-C3-C4	119.18	119.41	119.25	119.44	119.28	-
C2-C3-H7	120.03	119.92	120.12	119.9	120.09	-
C4-C3-H7	120.77	120.66	120.62	120.65	120.61	-
C3-C4-C5	121.13	121.47	121.41	121.45	121.38	-
C3-C4-N12	119.43	119.29	119.31	119.29	119.32	-
C5-C4-N12	119.43	119.22	119.26	119.25	119.28	-
C4-C5-C6	119.1	118.67	118.77	118.63	118.73	-
C4-C5-H8	120.82	120.97	120.95	120.98	120.97	-
C6-C5-H8	120.06	120.35	120.26	120.37	120.28	-
C1-C6-C5	122.2	122.5	122.46	122.58	122.55	-
C1-C6-N15	120.85	120.19	120.28	120.08	120.15	-
C5-C6-N15	116.94	117.3	117.25	117.32	117.28	-
C2-N9-O10	116.22	116.35	116.29	116.31	116.26	-
C2-N9-O11	117.98	117.81	117.52	117.67	117.41	-
O10-N9-O11	125.75	125.8	126.15	125.98	126.3	-
C4-N12-O13	117.29	117.24	117.18	117.17	117.12	-
C4-N12-O14	117.16	117.17	117.07	117.08	117	-
O13-N12-O14	125.53	125.58	125.74	125.73	125.87	-
C6-N15-O16	118.16	118.95	118.84	118.99	118.91	-
C6-N15-O17	117.89	117.87	117.54	117.72	117.41	-
O16-N15-O17	123.93	123.17	123.6	123.28	123.66	-
C1-O18-H19	110.76	106.52	107.05	106.08	106.42	-

Table 10: Observed and calculated dihedral of picric acid

Geometrical parameters bond angle (Å)	Methods				
	HF	B3LYP		B3PW91	
	6-311G (d,p)	6-31G (d,p)	6-311G (d,p)	6-31G (d,p)	6-311G (d,p)
C6-C1-C2-C3	1.466	1.3076	1.149	0.8878	1.151
C6-C1-C2-N9	-178.32	-178.85	-178.77	-178.8	-178.7

O18-C1-C2-C3	-176.45	-177.36	-177.18	-177.3	-177.1
O18-C1-C2-N9	3.7576	2.9185	2.8913	2.9281	2.925
C2-C1-C6-C5	-0.0635	0.3338	0.1648	0.3803	0.219
C2-C1-C6-N15	-179.74	-179.53	-179.55	-179.4	-179.5
O18-C1-C6-C5	177.72	178.516	178.428	178.54	178.46
O18-C1-C6-N15	-1.955	-1.3538	-1.2911	-1.331	-1.27
C2-C1-O18-H19	178.52	178.269	178.052	178.21	178.04
C6-C1-O18-H19	0.8105	0.1744	-0.1351	0.1478	-0.117
C1-C2-C3-C4	-2.032	-1.5772	-1.8541	-1.662	-1.923
C1-C2-C3-H7	178.18	178.319	177.9	178.24	177.89
N9-C2-C3-C4	177.76	178.152	178.075	178.1	178
N9-C2-C3-H7	-2.014	-1.9507	-2.1694	-1.99	-2.181
C1-C2-N9-O10	-145.8	-152.28	-146.7	-151.8	-146
C1-C2-N9-O11	36.25	29.2751	35.0592	29.729	35.55
C3-C2-N9-O10	34.382	27.9808	33.3687	28.386	33.86
C3-C2-N9-O11	-143.5	-150.45	-144.87	-150	-144.3
C2-C3-C4-C5	1.1688	1.0898	1.2392	1.178	1.3193
C2-C3-C4-N12	-178.9	-179.13	-179.09	-179	-179
H7-C3-C4-C5	-179	-178.8	-178.51	-178.7	-178.4
H7-C3-C4-N12	0.8001	0.9706	1.1482	1.0071	1.1373
C3-C4-C5-C6	0.1782	0.0726	0.026	0.0477	0.0006
C3-C4-C5-H8	179.71	179.675	179.622	179.63	179.58
N12-C4-C5-C6	-179.6	-179.7	-179.63	-179.6	-179.6
N12-C4-C5-H8	-0.132	-0.1012	-0.0404	-0.105	-0.052
C3-C4-N12-O13	-179.4	-179.51	-179.32	-179.4	-179.2
C3-C4-N12-O14	0.5989	0.4985	0.6989	0.527	0.747
C5-C4-N12-O13	0.4134	0.266	0.3458	0.256	0.364
C5-C4-N12-O14	-179.5	-179.71	-179.63	-179.7	-179.6
C4-C5-C6-C1	-0.729	-0.7932	-0.7334	-0.837	-0.777
C4-C5-C6-N15	178.96	179.08	178.994	179.03	178.96
H8-C5-C6-C1	179.72	179.601	179.667	179.57	179.63
H8-C5-C6-N15	-0.582	-0.5251	-0.6049	-0.547	-0.615
C1-C6-N15-O16	-178.4	-178.65	-178.31	-178.64	-178.3
C1-C6-N15-O17	1.6025	1.4008	1.7265	1.415	1.743
C5-C6-N15-O16	1.8929	1.4677	1.9512	1.477	1.946
C5-C6-N15-O17	-178	-178.47	-178	-178.46	-178

The vibrational wave numbers, IR intensity Raman intensity mode of vibration and polarization vector of picric acid have also been calculated by these authors who have been summarized in Table 11.

**Table 11: The observed and calculated vibrational wave numbers, IR intensity Raman intensity mode of vibration and polarization vector of picric acid**

S. No.	Symmetrical species (CS)	observed		methods				Vibrational assignments		
		Frequency (cm <sup>-1</sup> )		HF	B3LYP		B3PW91			
		FTIR	FT Raman		6-31+G (d,p)	6-311+G (d,p)	6-31+G (d,p)			6-311+G (d,p)
1	A'	3300 w	-	3295	3255	3327	3336	3292	(O-H)	υ
2	A'	2960 vs	-	2995	2959	2979	2957	2950	(C-H)	υ
3	A'	2950 vs	-	2988	2955	2975	2954	2946	(C-H)	υ
4	A'	-	1640 vs	1649	1665	1648	1648	1633	(C=C)	υ

5	A'	-	1630 vs	1634	1638	1619	1629	1610	(C=C)	υ
6	A'	1620 vs	-	1616	1622	1632	1617	1597	(C=C)	υ
7	A'	1550vs	-	1552	1555	1548	1575	1564	(N-O)	υas
8	A'	1540 vs	-	1540	1539	1531	1561	1551	(N-O)	υas
9	A'	-	1475 s	1460	1455	1468	1474	1459	(N-O)	υas
10	A'	1450 vs	-	1449	1452	1432	1426	1455	(C-C)	υ
11	A'	-	1445 vs	1447	1435	1448	1452	1440	(C-C)	υ
12	A'	-	1440 vs	1441	1427	1411	1455	1440	(C-C)	υ
13	A'	1420vs	-	1420	1416	1398	1443	1429	(N-O)	υs
14	A'	1340w	1340vs	1324	1336	1351	1317	1344	(N-O)	υs
15	A'	1310 vs	-	1311	1309	1319	1292	1314	(N-O)	υs
16	A'	1250 vs	-	1206	1258	1250	1266	1290	(O-H)	υ
17	A'	1180 m	-	1185	1175	1187	1157	1180	(C-H)	υ
18	A'	-	1150 vs	1168	1154	1145	1119	1150	(C-H)	υ
19	A'	1090 vs		1094	1994	1091	1091	1090	(C-N)	υ
20	A'	1085 vs	1085 vs	1048	997	995	993	991	(C-N)	υ
21	A'	950 m	-	991	947	960	923	945	(C-N)	υ
22	A'	-	940 m	959	937	950	919	938	(C-O)	υ
23	A''	-	920 vs	941	914	931	903	928	(C-H)	υ
24	A''	835 m	-	851	840	849	816	845	(C-H)	υ
25	A''	830 m	830m	828	837	840	809	830	(O-H)	υ
26	A'	-	800vs	806	793	809	803	818	(NO <sub>2</sub> )	υ
27	A'	-	795 s	785	798	797	807	791	(NO <sub>2</sub> )	υ
28	A'	780 vs	-	768	160	760	782	770	(NO <sub>2</sub> )	υ
29	A'	740 vs	740 s	735	757	744	766	737	(CCC)	υ
30	A'	730 vs	730 vs	725	756	728	761	726	(CCC)	υ
31	A'	700 vs	700 vs	704	733	703	738	714	(CCC)	υ
32	A'	-	660w	661	719	688	723	646	(C-N)	υ
33	A'	650 w	-	647	670	647	673	650	(C-N)	υ
34	A'	550 w	550 w	541	560	548	561	550	(C-N)	υ
35	A''	-	530 w	525	858	533	516	533	(NO <sub>2</sub> )	υ
36	A''	510 w	-	506	515	511	508	514	(NO <sub>2</sub> )	υ
37	A''	420 m	-	435	461	410	433	408	(NO <sub>2</sub> )	υ
38	A''	400 m	400 m	396	412	402	388	403	(CCC)	υ
39	A''	360 w	-	372	390	349	365	363	(CCC)	υ
40	A''	340 m	340w	344	355	338	333	342	(CCC)	υ
41	A'	330 w	-	336	351	332	329	336	(C-O)	υ
42	A''	320 m	-	322	333	321	312	323	(C-N)	υ
43	A''	310 m	310 w	310	324	310	303	311	(C-N)	υ
44	A''	200 m	200 m	198	207	198	195	199	(C-N)	υ
45	A''	190 w	-	183	192	188	192	188	(C-O)	υ
46	A''	150 w	150 m	154	158	150	148	153	(C-N)	υ
47	A''	120 w	-	124	131	121	131	125	(C-N)	υ
48	A''	110 w	-	88	101	97	102	96	(C-OH)	υ
49	A''	105 w	-	53	62	60	62	60	(NO <sub>2</sub> )	υ
50	A''	100 w	100 w	52	57	53	57	52	(NO <sub>2</sub> )	υ
51	A''	90 w	-	49	46	51	46	51	(NO <sub>2</sub> )	υ

Experimental and calculated <sup>1</sup>H and <sup>13</sup>C NMR chemical shift (ppm) of Picric acid have been summarized in Table 12.

Table 12: Experimental and calculated  $^1\text{H}$  and  $^{13}\text{C}$  NMR chemical shift (ppm) of picric acid

Atom position	Solvent DMSO		
	B3LYP/6-311+G(d,p) (ppm)	B3LYP/6-311+G (2d,p) (ppm) GIAO (ppm)	Shift
C1	11.04	188.94	177.9
C2	40.02	159.95	119.93
C3	44.6	155.38	110.78
C4	35.61	164.36	128.75
C5	45.3	154.68	109.38
C6	38.84	161.13	122.29
N9	142.52	400.92	258.4
N12	143.74	402.14	258.4
N15	144.99	403.39	258.4
O10	358.2	678.2	320
O11	419.78	739.78	320
O13	354.19	674.19	320
O14	354.47	674.47	320
O16	385.78	695.88	310.1
O17	331.81	651.81	320
O18	171.58	148.42	23.16
H7	22.59	9.29	13.3
H8	22.7	9.18	13.52
H19	22.03	8.84	13.19

The calculated energy values, chemical hardness, electro negativity, chemical potential and electrophilicity index of picric acid in gas phase from UV-Visible have been summarized in Table 13 and electronic absorption spectra of PA (absorption wavelength  $\lambda(\text{nm})$ , excitation energies  $E$  (eV) and oscillator strengths ( $f$ ) using TD-DFT/B3LYP/6-311++G(d,p) method gas phase in Table 14.

Table 13: Calculated energy values, chemical hardness, electro negativity, chemical potential and electrophilicity index of picric acid in gas phase

TD-DFT/B3LYP/6-311G++ (d,p)	2,4,6-trinitophenol
311G++ (d,p)	-
$E_{\text{total}}$ (Hartree)	568.59
$E_{\text{HOMO}}$ (eV)	8.363
$E_{\text{LUMO}}$ (eV)	4.296
$\Delta E_{\text{HOMO-LUMO}}$ gap (eV)	4.067
$E_{\text{HOMO-1}}$ (eV)	8.865
$E_{\text{LUMO+1}}$ (eV)	3.91
$\Delta E_{\text{HOMO-1-LUMO+1}}$ gap (eV)	4.955
Chemical hardness( $\eta$ )	2.033
Electronegativity ( $\chi$ )	3.315
Chemical potential ( $\mu$ )	6.329
Chemical softness ( $\sigma$ )	0.491
Electrophilicity index ( $\omega$ )	9.851
Dipole moment	1.837

**Table 14: Electronic absorption spectra of picric acid (absorption wavelength  $\lambda$ (nm), excitation energies E(eV) and oscillator strengths (f) using TD-DFT/B3LYP/6-311++G(d,p) method gas phase**

2,4,6-trinitrophenol			Gas	Assignment	Region
$\lambda$ (nm)	E (eV)	(f)	major contribution		
418.51	2.962	0.001	H→L (86%)	-	Visible
374.54	3.310	0.001	H→L (86%)	$n \rightarrow \pi^*$	Quartz UV
370.89	3.342	0.00	H→L (86%)	$n \rightarrow \pi^*$	Quartz UV

Ramalingam *et al.* [20] have also reported dipole moments  $\mu$  (D), the Polarizability  $\alpha$  (a.u.), the average Polarizability  $\alpha_0$  (esu), the anisotropy of the Polarizability  $\Delta\alpha$  (esu), the first hyperpolarizability  $\beta$  (esu) and thermodynamic properties at different temperatures on the B3LYP/6-311+G(d,p) level for TNP. Srivastava *et al.* [21] has carried out theoretical study on the site reactivity of picric acid and as reported the calculated values of various global and local properties of picric acid. The results of the calculations of surface properties and stock holder, Mulliken and electrostatic potential calculated by them also appear in the same paper. The visuals of different types of surfaces obtained by Srivastava *et al.* [21] appeared in Figure 4.

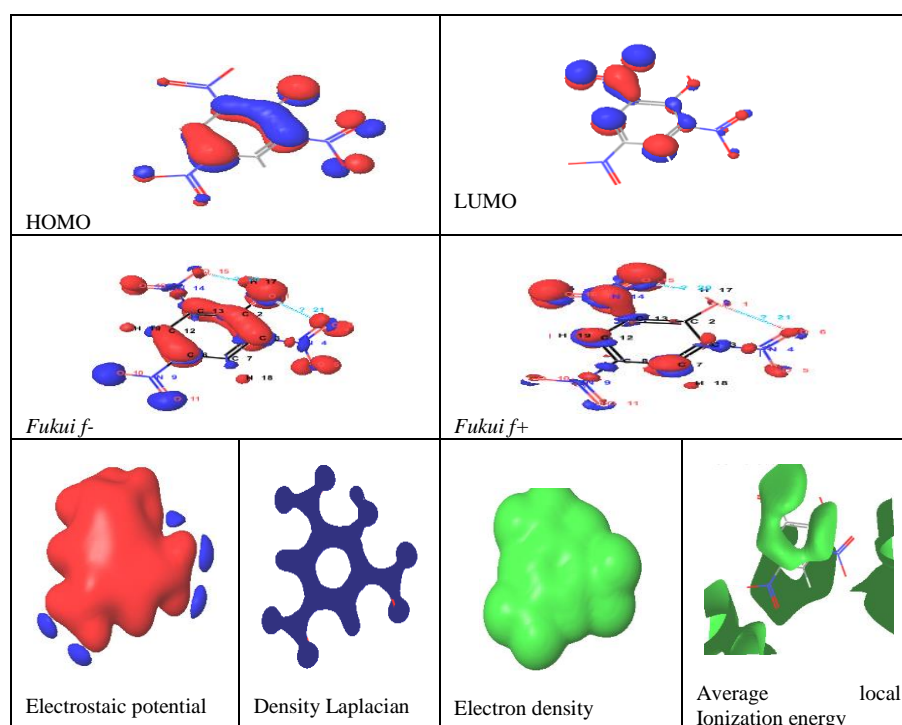


**Figure 4: Surface of HOMO, LUMO, Fukui functions, electrostatic potential, density laplacian, electron density and average local ionization energy of Picric acid calculated by DFT-B3LYP/6-31G\*\* level**

The HOMO is spread over whole molecule however the shifting of LUMO can be noticed in the figure of the LUMO. Srivastava *et al.* [22] have also reported the effect of different solvents on the global and local and various thermodynamic properties of Picric acid. Srivastava *et al.* [23] have also studied theoretically the druggability of picric acid and have reported their findings.

#### Analytical test in soil and water

##### Analysis in soil

Qualitative test of the presence of picric ion in soil is done by passing a soil extract to pass through a solid phase ion exchange column ie Alumina-A solid phase, anion exchange cartridge which retains picrate but not most yellowish interferences.

The column is then eluted with acetone solution containing 2% sulfuric acid which converts the picrate to colourless, undissociated picric acid. The eluted solution then filtered through a millexSR syringe filter place on the top of the cartridge, then diluted with water until the pH is above pKa of picric acid, this again produces yellow picrate anion which is visually detected [24]. The method can be performed, for example, as follows: Place 20 g of soil in a plastic bottle, add 100 ml of acetone and shake for 3 min. Filter 30 ml of acetone extract and measure the absorbance at 400 nm. If the absorbance is greater than 1.0, dilute the extract with acetone. Mix the filtered or diluted extract with an equal volume of water and pass the mixture through an Ahrmina-A SPE cartridge. Rinse the cartridge with methanol followed by acetone. Elute the picric acid with 10 ml of acidified acetone and measure the absorbance at 400 nm. Record the value as "Initial ABS." Dilute the acidified acetone eluent with 5 ml of unacidified acetone followed by 5 ml of water. Note any change in color and measure the absorbance at 400 nm. Record the value as "Final ABS." Calculate the quantity of picrate in the soil, expressed as picric acid:

$$\text{Kg g}^{-1} = \text{rf} \times [\text{final ABS} - 0.5 \times (\text{initial ABS})] \times \text{df}$$

Where  $\text{rf} = 50 \text{ Kg g}^{-1} \times [\text{final ABS} - 0.5 \times (\text{initial ABS})]$  is the daily response factor and  $\text{df}$  = the dilution factor, if used in step iii.

### Forensic analysis

Forensic analysts have been required to identify and quantify picric acid in complex mixtures of other nitro aromatic explosives. Paper chromatography [25] or thin layer chromatography [26] were used to separate picric acid from other explosives, where it was detected by color-forming reagents. Quantification was possible using a photodensitometer [27].

### Biological degradation

Lenke *et al.* [28] investigated the catabolic reactions of picric acid by the organisms *Rhodococcus erythropolis* strains HL24-A and HL-2. The catabolism of 2,4-dinitrophenol (2,4-DNP) by these micro-organisms were reported previously [29]. These authors found that the enzymes of the pathway adopted for the degradation of 2,4-DNP also attack picric acid. They observed that neither of the strains *R. erythropolis* HL 24-1 and HL-24-2 could utilize picric acid as a sole source of nitrogen, but the mutant strain *R. erythropolis* HL PM-1 utilized picric acid as a sole source of nitrogen. Picric acid was catabolized both under aerobic and anaerobic conditions; was rather low. In aerobic catabolism of picric acid the metabolites nitrate, 2,4-DNP and the dead end metabolite 1,3,5-trinitropentane were detected, while in anaerobic degradation 4,6-dinitro hexanoate was also detected. The proposed mechanism for nitrite elimination was suggested as shown in Figure 5 while formation of 1,3,5-trinitropentane was suggested as shown in Figure 6.

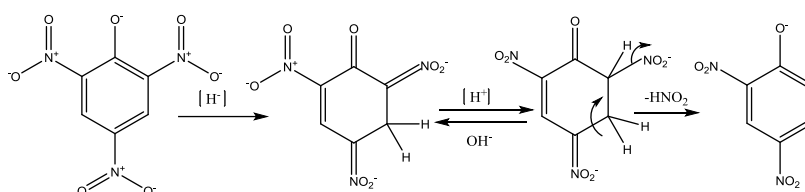


Figure 5: Proposed mechanism for nitrite elimination from picric acid

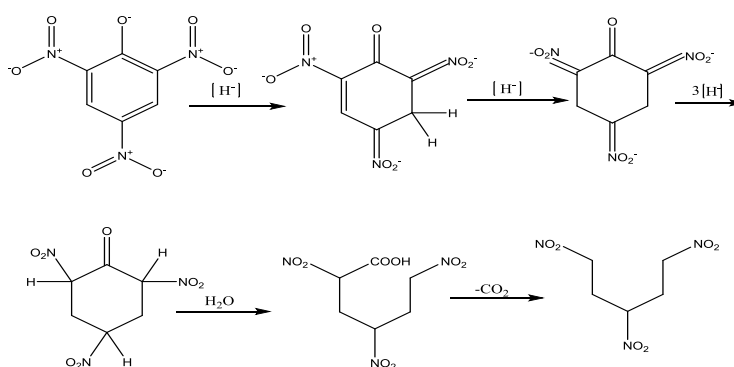


Figure 6: Hypothetical mechanism of the formation of 1,3,5- trinitro pentane

### Charge transfer complexes

Charge-transfer complexes are known to take part in many chemical reactions like addition, substitution and condensation [30,31]. These complexes have great attention for non-linear optical materials and electrical conductivities [32-35]. Electron donor-acceptor CT-interaction is also important in the field of drug-receptor binding mechanism [36], in solar energy storage [37] and in surface chemistry [38] as well as in many biological fields [39]. On the other hand, the CT-reactions of certain  $\pi$ -acceptors have successfully utilized in pharmaceutical analysis [40]. For these wide applications extensive studies on CT-complexes of  $\pi$ -acceptors have been performed [41].

Picric acid forms crystalline picrates of various organic molecules through ionic and hydrogen bonding and  $\pi$ - $\pi$  interactions and the presence of phenolic OH in the picric acid favors the formation of the salts with various organic bases [42]. The formation of charge transfer complex depending on the nature of the donor-acceptor system and the orientation of anionic and cationic species facilitates the formation of expected N-H...O hydrogen bonds between amino hydrogen and phenolic oxygen [43].

It has been reported that intramolecular hydrogen bonding interactions are absent in most of the picrate salts [44] and picric acid derivatives are interesting candidates, as the presence of phenolic OH and electron withdrawing nitro groups favors the formation of salts with various organic bases such as N,N-dimethylanilinium picrate [42], 3-Methyl aniliniumpicrate [43], 2-Chloroanilinium picrate [44], anilinium picrate [45], p-toluidinium picrate [44], 8-hydroxyquinolinium picrate [46], 1,3-Dimethylurea dimethyl ammonium picrate [47], N,N-Dimethyl anilinium picrate [48] have already been reported Priyadarshini *et al.* [49] have studied Synthesis, Growth, crystal structure and characterization of the o-Toluidinium picrate. They have carried out  $^1\text{H}$   $^{13}\text{C}$ -NMR, FTIR, single crystal X-ray diffraction, UV-VIS NIR transmission and fluorescence emission studies. Picric acid forms crystalline picrates of various organic molecules through ionic, hydrogen bonding and  $\pi$ - $\pi$  interactions [50]. It is known that picric acid acts not only as an acceptor to form various  $\pi$  stacking complexes with other aromatic molecules but also as an acidic ligand to form salts through specific electrostatic or hydrogen bond interactions [51]. Bonding of electron donor/acceptor picric acid molecules strongly depends on the nature of the partners. The linkage could involve not only electrostatic interactions but also the formation of molecular complexes [52]. Many new organic crystals have been examined based on the predictive molecular engineering approach and have been shown to have potential applications [53]. Other advantages of organic compounds involve amenability for synthesis, multifunctional substitution, higher resistance to optical damage and maneuverability for device application *et c.* [54].

Molecular flexibility of organic materials is an added advantage to enhance the nonlinear optical properties in a desired manner [55]. In addition, they have large structural diversity. By adopting molecular engineering methods in chemical synthesis one can easily refine the optical properties of organic molecules [56]. Picric acid forms crystalline picrate salts with various organic molecules by virtue of its acidic nature and forms salts through specific electrostatic or hydrogen bonding interactions [57].

The various organic sub-networks induce non-centrosymmetry in the bulk and enhance the thermal and mechanical stabilities through hydrogen bonding interactions [58,59].

Kraus and Fassel [18] have prepared forty picrates, reported their i.r. spectra and have classified under following groups. Group I.  $\pi$ - $\pi$ : Aromatic hydrocarbon single broad peak of  $\text{NO}_2$  group (asy) greater in frequency the  $1525\text{ cm}^{-1}$  and C-H one of plane bonded lower than  $783.5$ . Group II: Show two  $-\text{NO}_2$  (asy) one equal to or greater than that of PA and other at considerably lower frequency. C-H out of plane body scatters around  $783.5$ . These class of complexes contain aromatic hydrocarbon containing electron donating group such as  $\text{CH}_3$ ,  $-\text{OCH}_3$ ,  $-\text{OH}$ ,  $-\text{NH}_2$  etc.,  $\pi$ - $\pi$  + localized intermolecular interaction. In this complex one  $-\text{NO}_2$  is differentiated due to larger interaction with the donor.

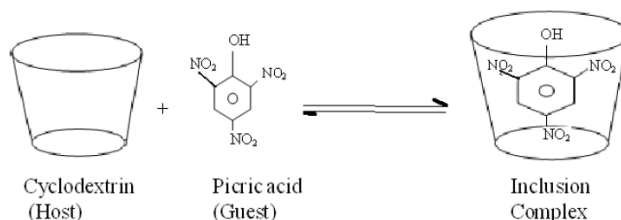
Group III: Two  $-\text{NO}_2$  asymmetric stretching more intense at the region of  $1525\text{ cm}^{-1}$  of PA and other the weaker are at higher frequencies  $\sim 1545\text{ cm}^{-1}$  out of plane bending appears at higher frequencies. The donor  $n$ - $\pi$ -\*containing  $n$ -donor atom closer proximity, greater interaction stability Srivastava *et al.* [60] have carried out DFT calculation at B3LYP-3 Level of theory with 6-311 G## basis set on the molecular interactions between *o*-phenanthroline and picric acid both in neutral molecular state and ionic state. They have reported that the interactions between molecules in ionic states are 21 times higher than the interactions in unionized state. They have also reported the visuals of the two kinds of interactions.

Srivastava *et al.* [61] have also carried out Theoretical investigation on the interactions between some indolyl Schiff's bases and picric acid in CT-complexes. They carried out computational study on the interactions of picric acid with some indolyl Schiff's bases having four different interaction sites by DFT method both in neutral and ionic states, the geometry of the resulting charge transfer complex, the actual site of interaction, nature of interactions and counterpoise corrected binding energies, etc. have been determined. They observed that interaction in the ionic state was found to be much stronger than the corresponding molecules in the neutral states and also reported the preferential site of interactions.

Priyadarshini *et al.* [62] have studied synthesis, growth, crystal structure and characterization of the *o*-toluidinium picrate. They have carried out  $^1\text{H}$   $^{13}\text{C}$ -NMR, FTIR, single crystal X-ray diffraction, UV-VIS NIR transmission and fluorescence emission studies.

#### Inclusion complex

Gopalan *et al.* [63] have prepared inclusion complex of picric acid in  $\beta$ -cyclodextrine which increases the solubility of PA in water. The bioavailability of picric acid increases in this type of complex. Under alkaline condition the complex becomes unstable. The proposed model of the inclusion equilibrium for picric acid- $\beta$ -Cyclodextrin complex.



#### CONCLUSION

Picric acid is known for about three and half centuries as a synthetic chemical. This explosive material can be stored safely in water as it explodes in dry state and on mechanical stress. It has wide spectrum of uses. Its toxicological and bio-degradational route, donor-acceptor behaviour, theoretical and experimental physico-chemical behaviour are also documented. All kinds of spectral data-both experimental and theoretical- are also available in the literature. Field methods for quantification of picric acid in soil and water samples have also been documented. The instant review also reports bond lengths, bond angles, dihedral angles, visuals of HOMO & LUMO, global & local properties, fukui indices, and drug ability studied on the basis of computational studies.

#### REFERENCES

- [1] W. Peter, *Philosophical Transactions of the Royal Society of London.*, **1771**, 61, 114130, 127130,
- [2] A. Laurent, *Annales de Chimie et de Physique. Series.*, **1841**, 221-228.
- [3] M.J. Briggs, B.T. Nguyen, L.W. Jorgensen, *J. Phys. Chem.*, **1991**, 95, 3315-3322.
- [4] M.E. Wolff, *Burger's Medicinal Chemistry and Drug Discovery*, 5<sup>th</sup> ed., New York: Wiley-Interscience, **1996**, 5537.
- [5] OSHA, Safety and Health Topics - Picric Acid, **2010**.
- [6] E.K. Weisburger, C.H. Powell, *Patty's Toxicology*, CD-ROM, **2001**.
- [7] National Research Council, *Drinking Water & Health*, Volume 4, Washington, DC., **1981**, 239.
- [8] R. Meyer, *Explosives*, VCH Verlagsgesellschaft mb, H. Weinheim, Germany, **1980**, 269-271.
- [9] P. Pfeiffer, *Organische Molekulverbindungen*, 2<sup>nd</sup> Edn., Ferdinand Enke, Stuttgart, **1927**.
- [10] Bingham, Eula, Cohrssen, Barbara, Powell, Charles, H. *Patty's Toxicology*, 5<sup>th</sup> Edn., John Wiley and Sons: NY, USA, **2001**.
- [11] A.S. Gaballa, C. Wagner, S.M. Tebeb, E.M. Nour, M.A.F. Elmosallamy, G.N. Kaluderovic, H. Schmidt, D. Steinborn, *J. Mol. Structure.*, **2008**, 876, 301.
- [12] A.M. Hindawey, A.M.G. Nassar, R.M. Issa, Y.M. Issa, *Indian J. Chem.*, **1980**, 19, 615-619.

- [13] H.A. Dessouki, M. Gaber, R. M. Issa, E.E. Hossani, *J. Indian Chem. Soc.*, **1988**, 258-262.
- [14] S.M. Refat, *J. Mol. Structure.*, **2011**, 985, 380-390.
- [15] G.A. Babu, S. Sreedhar, S.V. Rao, P. Ramasamy, *J. Cryst. Growth.*, **2010**, 312, 12-13, 1957-1962.
- [16] J.F. Wyman, M.P. Serve, D.W. Hobson, L.H. Lee, D.E. Uddin, *J. Toxicol. Environ. Health.*, **1992**, 37, 313-327.
- [17] V. Kadiyala, J.C. Spain, *Appl. Environ. Microbiol.*, **1998**, 64, 2479-2484.
- [18] R.D. Kross, V.A. Fassel, *J. Am. Chem. Soc.*, **1957**, 5, 38-41.
- [19] M.L. Lewis, I.R. Lewis, P.R. Griffiths, *Vib. Spectrosc.*, **2005**, 38, 11-16.
- [20] S. Ramalingam, J. David Ebenezer, R. Raja, J. Prabakar, *J. Theor. Comput. Sci.*, **2014**, 1(2), 1-11.
- [21] K.K. Srivastava, S. Srivastava, Md. Tanweer Alam, Rituraj, *Int. J. Innov. Appl. Res.*, **2014**, 2(1), 19-34.
- [22] K.K. Srivastava, Shubha Srivastava, Md. Tanweer Alam, Rituraj, *Int. J. Chem. Tech. Res.*, **2014**, 6(1), 730-749.
- [23] K.K. Srivastava, S. Srivastava, Md. Tanweer Alam, Rituraj, *World J. Pharm. Sci.*, **2014**, 3(6), 1706-1719.
- [24] G. Deniges, *Chem. Abstr.*, **1923**, 18, 2858.
- [25] J. Barnabas, *Chem. Abstr.*, **1954**, 49, 10128.
- [26] D. Parihar, S.P. Sharma, K.C. Tewari, *J. Chromatogr.*, **1966**, 24, 230.
- [27] J.F. Wyman, H.E. Guard, W.D. Won, J.H. Quay, *Appl. Environ. Microbiol.*, **1979**, 37, 222.
- [28] H. Lenke, D.H. Pieper, C. Bruhn, H.J. Knackmuss, *Appl. Environ. Microbiol.*, **1992**, 58(9), 2933-2937.
- [29] H. Lenke, D.H. Pieper, C. Bruhn, H.J. Knackmuss, *Appl. Environ. Microbiol.*, **1992**, 58, 2928-2932.
- [30] E.M. Kosower, *Prog. Phys. Org. Chem.*, **1965**, 3, 81.
- [31] F.P. Fla, J. Palou, R. Valero, C.D. Hall, P. Speers, *JCS Perkin Trans.*, **1991**, 2, 1925.
- [32] F. Yakuphanoglu, M. Arslan, *Opt. Mater.*, **2004**, 27, 29.
- [33] F. Yakuphanoglu, M. Arslan, *Solid State Commun.*, **2004**, 132, 229.
- [34] F. Yakuphanoglu, M. Arslan, M. Kucukislamoglu, M. Zengin, *Solar Energy.*, **2005**, 79, 96.
- [35] B. Chakraborty, A.S. Mukherjee, B.K. Seal, *Spectrochim. Acta A.*, **2001**, 57, 223.
- [36] A. Korolkovas, *Essentials of Medical Chemistry*, 2<sup>nd</sup> Edn., Wiley, NY, USA, **1998**.
- [37] K. Takahasi, K. Horino, T. Komura, K. Murata, *Bull. Chem. Soc. Jpn.*, **1993**, 66, 733.
- [38] S.M. Andrade, S.M.B. Costa, R. Pansu, *J. Colloid Interf. Sci.*, **2000**, 226, 260.
- [39] A.M. Slifkin, *Charge-Transfer Interaction of Biomolecules*, Academic Press, New York, **1971**.
- [40] F.M. Abou Attia, *Farmaco.*, **2000**, 55, 659.
- [41] K. Basavaiah, *Farmaco.*, **2004**, 59, 315.
- [42] H. Takayanagi, T. Kai, S. Yamaguchi, K. Takeda, M. Goto, *Chem. Pharm. Bull.*, **1996**, 44(12), 2199-2204.
- [43] P. Ramesh, R. Akalya, A. Chandramohan, M.N. Ponnusamy, *Acta Crystallographica Section E.*, **2010**, 66, 4.
- [44] C. Muthamizhchelvan, K. Saminathan, J. Fraanje, R. Peschar, K. Sivakumar, *Anal. Sci.*, **2005**, 21(4), 61-62.
- [45] G. Smith, U.D. Wermuth, P.C. Healy, *Acta Crystallographica Section E*, **2004**, 60, 1800-1803.
- [46] V.K. Kumar, R. Nagalakshmi, *Spectrochimica Acta Part A.*, **2007**, 66(4-5), 924-934.
- [47] G. Anandha Babu, A. Chandramohan, P. Ramasamy, G. Bhagavannarayana, B. Varghese, *Mat. Res. Bull.*, **2011**, 46(3), 464-468.
- [48] A. Chandramohan, R. Bharathikannan, M.A. Kandhaswamy J. Chandrasekaran, R. Renganathan, V. Kandavelu, *Cryst. Res. Technol.*, **2008**, 43(2), 173-178.
- [49] S. Yamaguchi, M. Goto, H. Takayanagi, H. Ogura, *Bull. Chem. Soc. Jpn.*, **1988**, 61, 1026.
- [50] H. Nagata, M. Doi, T. Ishida, A. Wakahara, *Acta Crystallogr. C.*, **1997**, 5367.
- [51] P. Zaderenko, S.M. Gel, P. Lopez, P. Ballesteros, I. Fonseca, A. Albert, *Acta Crystallogr. B.*, **1997**, 53 961.
- [52] T. Mallik, T. Kar, *Mater. Lett.*, **2007**, 61, 3826.
- [53] Z.H. Sun, G.H. Zhang, X.Q. Wang, X.F. Cheng, X.J. Liu, L. Zhu, Y. Fan, G. Yu, D. Xu, *J. Cryst. Growth.*, **2008**, 310, 2842.
- [54] A. Datta, S.K. Pati, *J. Chem. Phys.*, **2003**, 118, 8420.
- [55] G. De Matos, V. Venkataraman, E. Nogueira, M. Belsley, P.A. Criado, M.J. Dianez, E.P. Garrido, *Synth. Met.*, **2000**, 115, 225.
- [56] D.S. Chemla, J. Zyss, *Nonlinear Optical Properties of Organic Molecules and Crystals*, New York, **1987**.
- [57] A. Criado, M.J. Dianez, S.P.L. Garrido, I.M. Fernandes, M.E. Belsley, M. De Gomes, *Acta Crystallogr.*, **2000**, 56, 888.
- [58] J. Zaccaro, J.P. Salvestrini, A. Ibanez, P. Ney, M.D. Fontana, *J. Opt. Soc. Am.*, **2000**, 17, 427.
- [59] K. Muthu, S. Meenakshisundaram, *J. Cryst. Growth.*, **2012**, 352(1), 163-166.
- [60] K.K. Srivastava, S. Srivastava, Md. Tanweer Alam, Rituraj, *Pelagia Res. Lib.*, **2015**, 6(1), 7-12.
- [61] K.K. Srivastava, S. Srivastava, Md. Tanweer Alam, Rituraj *Arch. Appl. Sci. Res.*, **2014**, 6(2), 67-75.
- [62] K.M. Priyadarshini, A. Chandramohan, T. Uma Devi, *J. Cryst. Process Technol.*, **2013**, 3, 123-129.
- [63] P.R. Gopalan, A.G. Anna Selvi, P. Subramaniam, *Int. J. Agric. Food Sci.*, **2013**, 3(3), 90-94.